Respiratory effort during sleep and prevalent hypertension in obstructive sleep apnoea

Jean-Benoit Martinot ●[1,2], Nhat-Nam Le-Dong[3], Atul Malhotra[4] and Jean-Louis Pépin[5]

[1]Sleep Laboratory, CHU Université Catholique de Louvain (UCL) Namur Site Sainte-Elisabeth, Namur, Belgium. [2]Institute of Experimental and Clinical Research, UCL Bruxelles Woluwe, Brussels, Belgium. [3]Sunrise, Namur, Belgium. [4]Division of Pulmonary, Critical Care, and Sleep Medicine, Department of Medicine, University of California San Diego, La Jolla, CA, USA. [5]HP2 Laboratory, Inserm U1300, University Grenoble Alpes, Grenoble, France.

Corresponding author: Jean-Benoit Martinot (martinot.j@respisom.be)

Abstract

Background Mechanisms underlying blood pressure changes in obstructive sleep apnoea (OSA) are incompletely understood. Increased respiratory effort is one of the main features of OSA and is associated with sympathetic overactivity, leading to increased vascular wall stiffness and remodelling. This study investigated associations between a new measure of respiratory effort (percentage of total sleep time spent with increased respiratory effort based on measurement of mandibular jaw movements (MJM): REMOV, %TST) and prevalent hypertension in adults referred for evaluation of suspected OSA.

Methods A machine learning model was built to predict hypertension from clinical data, conventional polysomnography (PSG) indices and MJM-derived parameters (including REMOV). The model was evaluated in a training subset and a test subset.

Results The analysis included 1127 patients: 901 (80%) in the training subset and 226 (20%) in the test subset. The prevalence of hypertension was 31% and 30%, respectively, in the training and test subsets. A risk stratification model based on 18 input features including REMOV had good accuracy for predicting prevalent hypertension (sensitivity 0.75 and specificity 0.83). Using the Shapley additive explanation method, REMOV was the best predictor of hypertension after clinical risk factors (age, sex, body mass index and neck circumference) and time with oxygen saturation <90%, ahead of standard PSG metrics (including the apnoea–hypopnoea index and oxygen desaturation index).

Conclusion The proportion of sleep time spent with increased respiratory effort automatically derived from MJM was identified as a potential new reliable metric to predict prevalent hypertension in patients with OSA.

Introduction

Obstructive sleep apnoea (OSA) is a highly prevalent condition [1] that is associated with a variety of adverse consequences, including excessive daytime sleepiness [2], cognitive dysfunction [3] and cardiovascular disease [4], especially hypertension [5–7].

The main acute physiological consequences of OSA are intermittent hypoxia, intrathoracic pressure changes generated by increased respiratory effort and arousals [8]. Increased respiratory effort is therefore a key component of obstructive apnoeas/hypopnoeas and respiratory effort-related arousals (RERAs). The apnoea–hypopnoea index (AHI) has traditionally been used to estimate OSA severity and describes the average number of respiratory events occurring per hour of sleep. However, the AHI does not convey relevant information about hypoxic burden and total sleep time (TST) spent with increased respiratory effort despite the fact that these metrics have been linked to OSA cardiovascular and mortality outcomes

[9, 10]. As a result, it is now widely accepted that the AHI is unable to capture fully the complex pathophysiological processes of OSA [11, 12], and that more comprehensive and combined metrics are required to define fully cardiovascular risk in a given patient with OSA.

The role of increased respiratory effort in cardiovascular mortality has been poorly studied to date. The only physiological data currently available show that intrathoracic pressure swings during respiratory events generate subsequent sympathetic nervous system overactivity [13, 14], and might accelerate arterial stiffness and arterial wall remodelling. In addition, currently available evidence suggests that respiratory effort contributes to increases in nocturnal blood pressure [15–25].

The lack of data on the cardiovascular impact of increased respiratory effort can be partly explained by the challenge of assessing and measuring the proportion of TST spent with increased respiratory effort. We have previously demonstrated that mandibular jaw movements (MJM) during sleep provide powerful information about respiratory effort and sleep time spent with increased respiratory effort [26, 27]. In normal physiological sleep, the mandibular jaw slightly moves a few tenths of a millimetre at the breathing frequency around a fixed position and the mouth is almost closed. This sleep physiological displacement is controlled by the respiratory and pre-motor trigeminal nuclei, and reflects respiratory drive and variations in respiratory efforts. MJM therefore reflects respiratory drive level and efforts as a function of variations in upper airway resistance that typically occur during abnormal respiratory events [26, 27].

This study evaluated the association between sleep time spent with increased respiratory effort automatically derived from measurements of MJM (REMOV, %TST) and prevalent hypertension in patients being investigated for suspected OSA. We hypothesised that an increase in MJM during sleep would be independently associated with hypertension beyond the classical metrics of hypoxic burden and sleep fragmentation.

Methods

Study design and population

This was a cross-sectional analysis of consenting consecutive adult patients referred for assessment of suspected OSA. The study was approved by the Comité d'Ethique Hospitalo-Facultaire-Universitaire de Liège (Liege, Belgium; IRB-00004890-NB707201523388) and all participants provided written informed consent prior to enrolment.

Overnight sleep study

In-laboratory polysomnography (PSG) was recorded with a digital acquisition system (SOMNOscreen Plus; SOMNOmedics, Randersacker, Germany). The parameters monitored included electroencephalogram (EEG), right and left electro-oculogram, submental electromyogram (EMG), tibial EMG, chest and abdominal wall motion by respiratory inductance plethysmography (SleepSense; SLP, St Charles, IL, USA), nasal and oral flows by a pressure transducer and a thermistor, respectively, and peripheral oxygen saturation (S_{pO_2}) by a digital oximeter displaying pulse waveform (Nonin Medical, Plymouth, MN, USA).

PSG recordings were manually scored by two experienced investigators who were unaware of participant identity. All sleep stages, EEG arousals and sleep-related respiratory events were visually scored based on American Academy of Sleep Medicine criteria [28, 29]. OSA diagnosis was confirmed based on International Classification of Sleep Disorders-3 criteria and required either signs/symptoms or related medical/psychiatric disorders together with ⩾5 predominantly obstructive respiratory events (*i.e.* obstructive and mixed apnoeas, hypopnoeas or RERAs; referred to as PSG_ORDI) per hour of sleep. Alternatively, occurrence of ⩾15 obstructive respiratory events per hour was sufficient to diagnose OSA, even in the absence of associated symptoms or disorders [30]. The conventional rules for severity grading based on AHI were used to categorise into non-OSA (<5 events·h^{-1}), mild (5–15 events·h^{-1}), moderate (15–30 events·h^{-1}) and severe (>30 events·h^{-1}) [12]. Interobserver agreement for PSG scoring was evaluated by the intraclass correlation coefficient using a two-way random model for single measures (ICC 2,1); this was 0.921 (95% CI 0.891–0.942; p<0.001).

MJM recordings

MJMs were recorded using the Sunrise system (Sunrise, Namur, Belgium). This is composed of a coin-sized tri-axial sensor including a gyroscope and an accelerometer that was attached to the patient's chin between the inferior labial sulcus and the pogonion by the sleep technician. The embedded inertial measurement unit enables MJM sensing and communicates with a smartphone application for external control. Displacement of the mandible is calculated from the rotational speed measured by the gyroscope.

The position of the mandible resulting from elevation or depression is determined by the accelerometer. This inertial measurement unit provides six derived channels in total.

MJM signal automated machine learning algorithms were trained with a large number of fragments obtained from periods of normal breathing and epochs that included the full spectrum of obstructive events (RERAs, obstructive apnoeas, obstructive hypopnoeas and mixed episodes) and central events. Details of absolute values generated by the Sunrise system have been reported previously [27].

MJM data were automatically transferred to a cloud-based infrastructure at the end of the night and data analysis was performed using a dedicated machine learning algorithm. This algorithm is designed to identify automatically obstructive and mixed apnoea/hypopnoea or RERA based on stereotypical MJM patterns. It automatically processes MJM signal components and determines whether MJM patterns could be classified as sleep, arousal or wake. To identify wake, the algorithm tested whether MJM signals were fast, irregular and non-predictable [31]. For the identification of arousal movements, the algorithm detected brisk MJM of large amplitude indicating the abrupt closure of the mouth characteristic of arousals [31, 32].

Respiratory effort burden

This new metric provides an indication of the time spent with increased respiratory effort assessed using MJM. Periods of increased respiratory effort were identified through oscillating MJMs of increased and variable amplitudes at the breathing frequency (figure 1) [26, 27]. The MJM algorithm identifies respiratory disturbances as a period with increased respiratory effort ended by an arousal or an awakening. The Sr_ORDI consists of the total number of respiratory disturbances accompanied by increased respiratory effort divided by TST, as estimated from the Sunrise analytics [33]. The new variable is increased respiratory effort during sleep based on MJM measurement as a proportion of TST (REMOV, %TST).
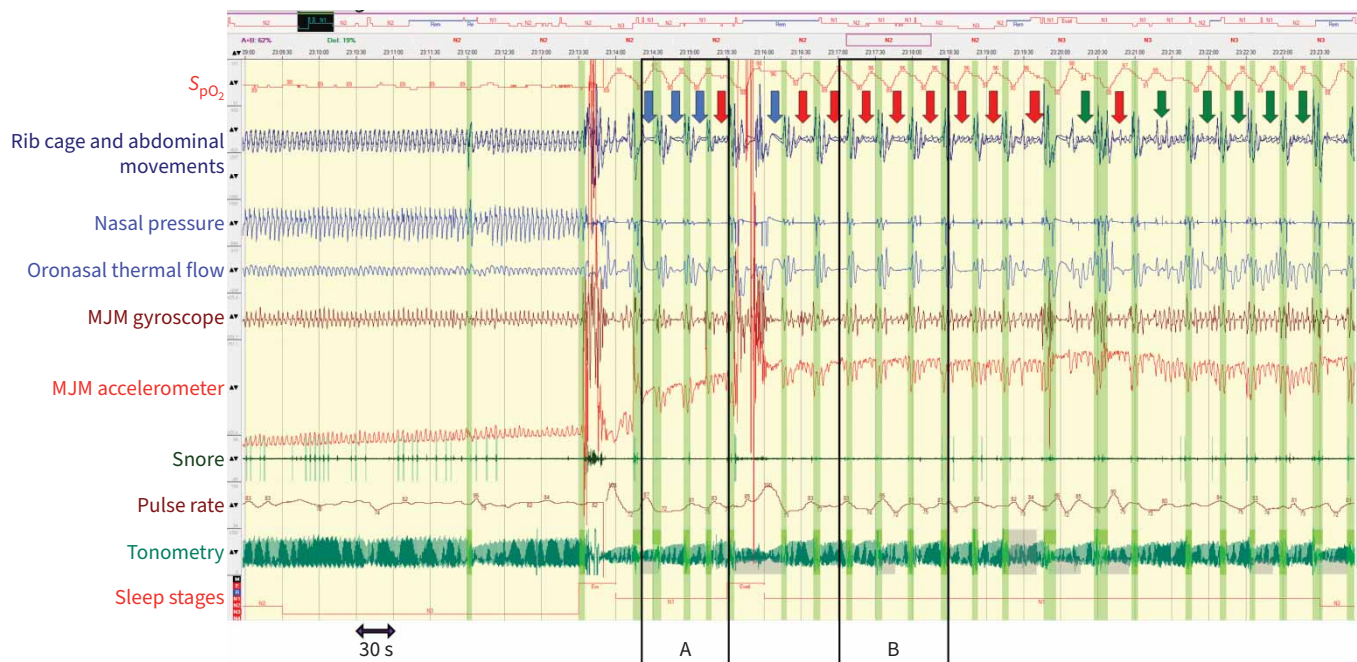

FIGURE 1 15-min fragment of recording showing mandibular jaw movements (MJM) during increased respiratory effort across sleep disordered breathing. From left to right, a typical period of respiratory effort-related arousal is seen during the first 4 min where inspiratory flow limitation is clearly seen on the nasal pressure channel with snoring while the abdomino-thoracic belts remain synchronous. The respiratory displacements of the mandible are well captured by the gyroscope and the accelerometer, showing a mild increase in respiratory effort. During periods of stable flow limitation, the amplitude of the mandibular displacement increases as a function of the intensity of effort. In contrast, after short awakening, there are successive central apnoeas (blue arrows). During central apnoeas, mandibular movements decrease dramatically and can disappear until arousal occurs. Then, there are obstructive apnoeas (red arrows) and hypopnoeas (green arrows) that are accompanied by a greater increase in respiratory effort (see amplitude of mandibular movements) in parallel with desynchronisation of the belts. Highlighted portions "A" and "B" are shown in more detail in supplementary figure S4a and b. S_{pO_2}: peripheral oxygen saturation.

Prevalent hypertension outcome

A sleep specialist performed a clinical examination in the morning (between 08:30 and 12:00) during which blood pressure was measured three times with the patient seated in a quiet room. All medications were recorded in an electronic medical record. History, office blood pressure and medication usage were used to define hypertension status. The presence of hypertension was defined as a documented history of hypertension and treatment with at least one antihypertensive drug.

Data analysis

Data preparation, exploratory analysis, model development, validation and interpretation were carried out using Python programming language. The data analytics plan is summarised in figure 2. Key elements are described in the following subsections.

Data splitting and optimisation of machine learning algorithm

The dataset was randomly divided into two subsets: a larger set for model development and a smaller set for secondary independent validation. We built a binary classification rule to recognise patients with comorbid hypertension based on input data for 18 anthropometric features and sleep studies indices: male sex (binary value), age, body mass index (BMI), neck circumference, Epworth Sleepiness Scale (ESS) score, nine PSG-derived indices (PSG_TST, respiratory disturbance index (PSG_RDI), obstructive RDI (PSG_ORDI), PSG_AHI, obstructive AHI (PSG_OAHI), oxygen desaturation index (ODI), arousal index (PSG_ArI) and proportion of TST spent with S_{pO_2} <90% or <95% (Desat_dt <90% and <95%)) and four indices provided by Sunrise's automatic MJM signal analysis (Sr_TST, Sr_ArI, Sr_ORDI and REMOV).

The extreme gradient boosting (XGB) classifier algorithm was adopted for this classification task (see supplementary material for more details). The learning objective is set as a binary classification, with hypertension as the positive label. The training implied a gradient tree booster and histogram-optimised approximate greedy tree construction algorithm.
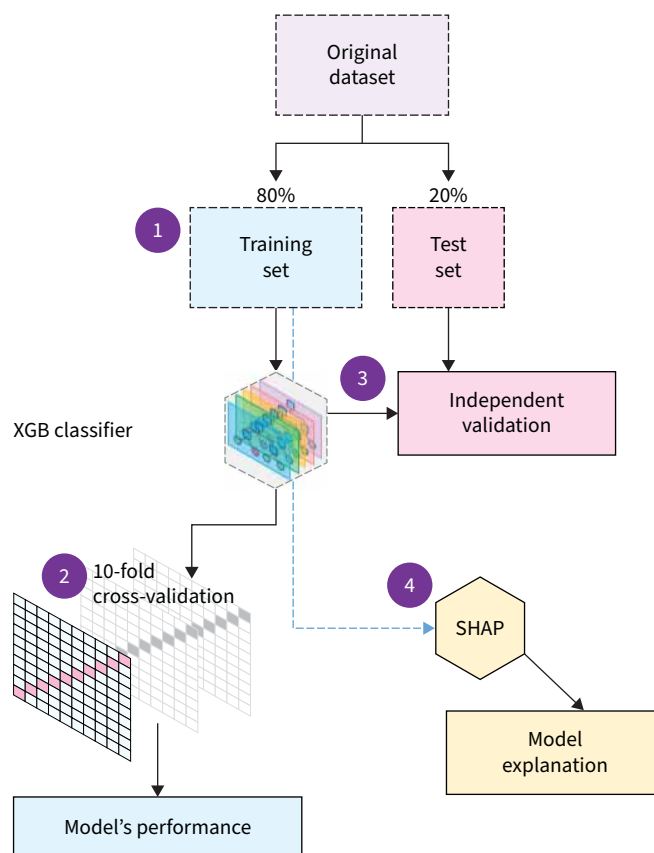

FIGURE 2 Overview of the experimental and analysis protocol. XGB: extreme gradient boosting; SHAP: Shapley additive explanation method.

Cross-validation on training set

The model's performance was evaluated using the 10-fold cross-validation procedure, which implied multiple data splitting and random resampling, thus allowing unbiased evaluation of model performance on 10% of unseen data.

Secondary validation on independent dataset

A final model was trained on the whole training subset using the optimised parameter values. This model was validated on unseen data in the testing subset. The following evaluations were conducted for both repeated 10-fold cross-validation and independent validation: normalised confusion matrix (to evaluate model accuracy; the rows represent the true observation and the columns indicate the classification by model) and conventional metrics for evaluating the binary classification accuracy and diagnostic efficiency, including sensitivity, specificity, F1 score (harmonic mean between sensitivity and positive predictive value), balanced accuracy, positive/negative likelihood ratios, positive predictive value, negative predictive value and area under the receiver operating characteristic curve (AUC).

Model explanation and evaluation of features contribution

To evaluate the contribution of each feature to the model final prediction, the Lundberg Shapley additive explanation (SHAP) method was applied [34]. This method unifies the concept of Shapley values from cooperative game theory (1953) with a local interpretation approach. The SHAP method allows depiction of the respective power of association of different factors on the explanatory variable (in this case hypertension). It also allows inclusion of all variables of interest even if collinearity exists between some of the variables.

The association between respiratory effort burden and the risk of comorbid hypertension was also explored using a conventional statistical inference based on regression coefficients from a 10-fold cross-validation of the Ridge logistic regression model. The model implies a linear regression with binomial distribution and a L2 regularisation, which provides more stable parameters.

Results

Study population

A total of 1127 subjects were included in the study: 901 (80%) in the training subset and 226 (20%) in the test subset (table 1). The prevalence of hypertension was 31% and 30%, respectively, in the training and test subsets. In the training subset, mean blood pressure was 136/82 mmHg in patients with hypertension and 128/78 mmHg in those without hypertension (table 1); six patients met the criteria for resistant hypertension. Patients with *versus* without hypertension differed in several clinical characteristics and respiratory parameters (table 1).

Clinical characteristics and respiratory effort burden

Clear differences in the distribution of a variety of features based on the presence or absence of hypertension (figure 3a) provide an indication of the potential for association between that feature and hypertension. The features were categorised by their pathophysiological characteristic and method of measurement (PSG ("PSG_") or Sunrise ("Sr_") system) and were combined with anthropometric parameters influencing blood pressure (as described in the Methods section).

The PSG-derived ORDI and ArI metrics distribution and the corresponding MJM-derived indices reflecting number of events and desaturation were similarly distributed between the groups with and without hypertension (figure 3a). Respiratory effort burden (REMOV, %TST) was higher in patients with *versus* without hypertension (figure 3a), suggesting a high ability of REMOV to differentiate between patients with and without hypertension. On principal component analysis, TST and the ESS score did not contribute to hypertension risk, whereas other respiratory measures and demographic/clinical features were associated with the presence of hypertension (figure 3b).

Machine learning model for predicting prevalent hypertension

A machine learning model including a variety of anthropometric parameters and physiological features from PSG and Sunrise technology showed good performance for the prediction of hypertension in the test subset (table 2). The final model showed good performance in the test subset, with AUC 0.88 (95% CI 0.85–0.90), sensitivity 0.75 (95% CI 0.66–0.83) and specificity 0.83 (95% CI 0.78–0.88) (figure 4 and table 2). A ROC without REMOV showed worse performance with respect to the sensitivity/specificity trade-off (supplementary figure S1 and supplementary table S1).

TABLE 1 Characteristics of the study population				
	Training subset (n=901 (80%))		Test subset (n=226 (20%))	
	Hypertension (n=279 (31%))	Without hypertension (n=622 (69%))	Hypertension (n=68 (30%))	Without hypertension (n=158 (70%))
Male	129 (46.2)	265 (42.6)	35 (51.5)	80 (50.6)
Age, years	56.58±15.72	44.17±18.24	55.06±13.03	44.57±17.70
Neck circumference, cm	41.00±5.00	39.00±5.00	40.00±3.00	39.00±5.00
Blood pressure				
Systolic, mmHg	135.7±17.1	128.0±12.4	138.4±22.3	125.4±14.5
Diastolic, mmHg	82.1±13.6	78.2±11.9	80.9±17.2	75.9±11.1
BMI, kg·m^{-2}	32.87±10.17	28.52±11.06	31.78±9.52	30.15±10.30
ESS score	11.00±8.00[#]	11.00±7.00	10.00±7.00[#]	11.00±6.00
OSA severity				
Non-OSA	19 (6.8)	104 (16.7)	4 (5.9)	27 (17.1)
Mild	49 (17.6)	223 (35.9)	13 (19.1)	57 (36.1)
Moderate	81 (29.0)	149 (24.0)	22 (32.4)	39 (24.7)
Severe	130 (46.6)	146 (23.5)	29 (42.6)	35 (22.2)
PSG indices				
TST, min	420.52±109.76[#]	437.27±98.12	415.76±76.13	430.75±89.87
ArI, events·h^{-1}	29.57±23.71	22.89±17.45	28.96±22.40	22.96±16.98
AHI, events·h^{-1}	27.32±29.12	14.00±22.31	26.52±27.90	14.04±19.64
OAHI, events·h^{-1}	19.44±27.99	9.87±19.23	19.18±26.45	9.26±16.71
RDI, events·h^{-1}	34.33±31.29	20.84±24.70	32.76±27.54	21.28±21.18
ORDI, events·h^{-1}	26.73±27.00	15.84±21.42	27.95±25.84	16.26±18.58
ODI, events·h^{-1}	24.86±35.26	10.73±23.01	23.87±32.97	9.54±20.94
Desat_dt <90%, %TST	3.43±12.90	0.28±3.06	4.35±9.73	0.36±3.79
Desat_dt <95%, %TST	19.45±22.40	7.63±16.03	17.88±21.80	7.38±15.35
Sunrise indices				
TST, min	439.00±81.25[#]	439.74±75.73	450.75±65.25	439.25±68.00
ORDI, events·h^{-1}	20.66±15.20	13.50±14.34	22.52±16.80	13.62±13.01
ArI, events·h^{-1}	21.97±16.16	17.79±13.55	23.35±21.42	17.24±13.69
REMOV, %TST	75.96±26.96	56.05±47.95	77.34±26.40	55.41±43.83
Antihypertensive medication				
β-blocker	127 (45.5)		54 (79.4)	
ACE inhibitor	79 (28.3)		38 (55.9)	
ARB	71 (25.4)		27 (39.7)	
CCB	87 (31.2)		14 (20.6)	
Diuretic	63 (22.6)		19 (27.9)	
Other	12 (4.3)		1 (1.5)	
Antihypertensives				
0		622 (100.0)		158 (100.0)
1	176 (63.1)		13 (19.1)	
2	52 (18.6)		31 (45.6)	
3	46 (16.5)		18 (26.5)	
4	4 (1.4)		6 (8.8)	
5	1 (0.4)			

Data are presented as n (%) or mean±SD. BMI: body mass index; ESS: Epworth Sleepiness Scale; OSA: obstructive sleep apnoea; PSG: polysomnography; TST: total sleep time; ArI: arousal index; AHI: apnoea–hypopnoea index; OAHI: obstructive apnoea–hypopnoea index; RDI: respiratory disturbance index; ORDI: obstructive respiratory disturbance index; ODI: oxygen desaturation index; Desat_dt <90% or <95%: proportion of TST spent with oxygen saturation <90% or <95%; REMOV: increased respiratory effort during sleep (based on mandibular jaw movements measurement); ACE: angiotensin-converting enzyme; ARB: angiotensin receptor blocker; CCB: calcium channel blocker. [#]: all metrics, except for TST (PSG and Sunrise) and ESS, showed a statistically significative difference in distribution between two outcome subgroups, based on a Mann–Whitney test at a significance threshold of 0.005.

Model explanation by SHAP method

The five strongest predictors of prevalent hypertension in patients with OSA were age, male sex, time with S_{pO_2} <90% (Desat_dt <90%), BMI and neck circumference (figure 5). The three next most important
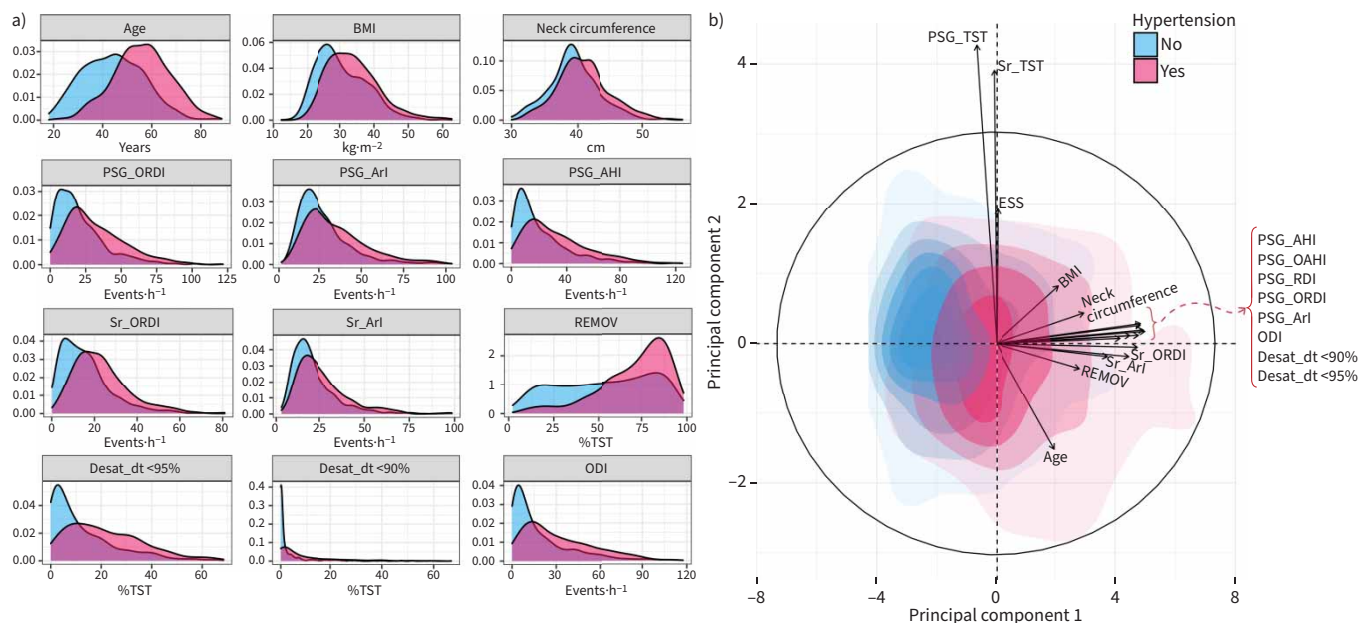
FIGURE 3 Distribution of clinical features and principal component analysis (PCA). a) Density plots showing the distribution of 12 features that showed the most significant difference between participants with or without hypertension. b) Loading plot summarising the PCA. The graph consists of a bi-dimensional density layer, representing the joint distribution of two principal components, and coordinates of the 17 original variables as vectors, including age, body mass index (BMI), neck circumference, Epworth Sleepiness Scale (ESS) score, nine PSG-derived indices (PSG_TST, respiratory disturbance index (PSG_RDI), obstructive RDI (PSG_ORDI), apnoea–hypopnoea index (PSG_AHI), obstructive AHI (PSG_OAHI), oxygen desaturation index (ODI), arousal index (PSG_ArI), proportion of TST spent with peripheral oxygen saturation (S_{pO_2}) <90% or <95% (Desat_dt <90% and <95%)) and four indices provided by Sunrise's automatic mandibular jaw movements signal analysis (Sr_TST, Sr_ArI, Sr_ORDI and REMOV). Each vector represents a variable; its orientation with respect to a principal component axis and length indicate how much the variable contributes to that principal component. The angles between the vectors and direction allow evaluation of their correlation: small angles indicate strong positive correlation; opposite angles represent a negative correlation.

contributors were REMOV, Sr_ORDI and PSG_ORDI (figure 5). These were followed by other PSG indices (in descending order of importance): PSG_TST, time with S_{pO_2} <95% (Desat_dt <95%), PSG_OAHI and PSG_ArI (figure 5).

Of these metrics, only REMOV and Sr_ORDI showed a clear asymmetric pattern in SHAP values distribution, where the highest values of REMOV and Sr_ORDI would drive positive prediction of hypertension. In contrast, SHAP values were cumulated at the centre for most PSG indices, indicating a

TABLE 2 Evaluation of model performance by repeated 10-fold cross-validation and independent validation on test subset

	Repeated 10-fold cross-validation (n=901)	Independent validation on test subset (n=226)
F1 score	0.76 (0.70–0.81)	0.70 (0.62–0.77)
Balanced accuracy	0.76 (0.71–0.81)	0.79 (0.74–0.84)
Sensitivity	0.77 (0.69–0.85)	0.75 (0.66–0.83)
Specificity	0.75 (0.67–0.83)	0.83 (0.78–0.88)
Positive predictive value	0.65 (0.56–0.74)	0.75 (0.67–0.82)
Negative predictive value	0.89 (0.84–0.93)	0.77 (0.70–0.87)
Positive likelihood ratio	3.17 (2.33–4.32)	4.52 (3.29–6.21)
Negative likelihood ratio	0.30 (0.19–0.40)	0.30 (0.19–0.41)
AUC	0.84 (0.79–0.89)	0.88 (0.85–0.90)

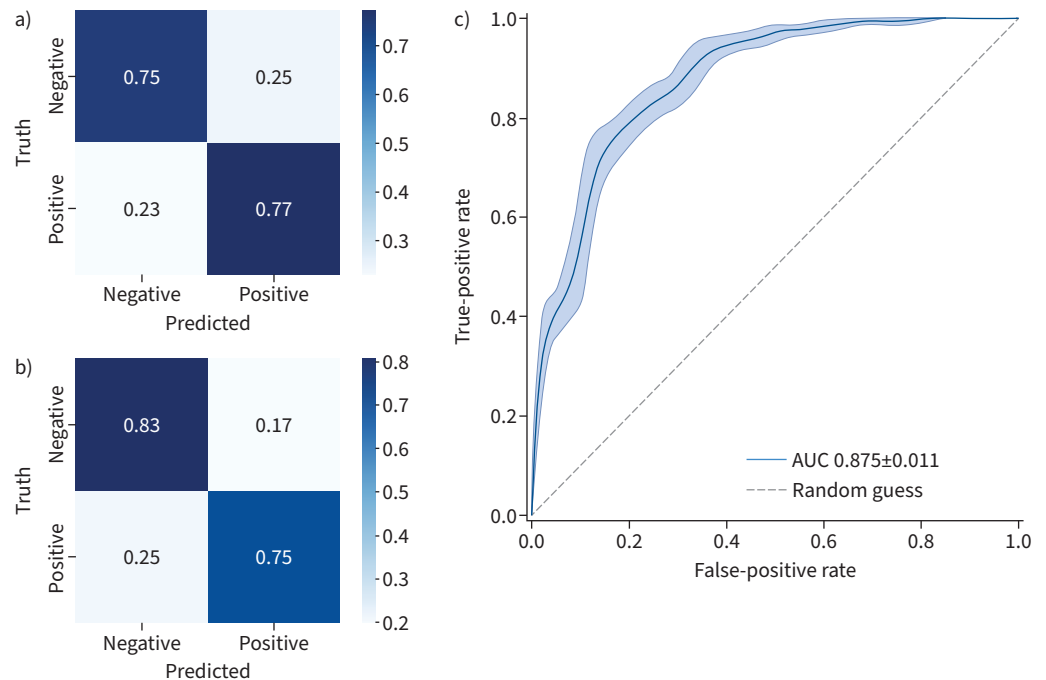Data are presented as estimate (95% CI). AUC: area under the receiver operating characteristic curve.

FIGURE 4 Global performance of the model based on repeated 10-fold cross-validation and independent data. a) Average normalised confusion matrix obtained from 100 replications of the extreme gradient boosting model in a 10-fold cross-validation. b) Normalised confusion matrix based on application of the final model on unseen data from 226 subjects. c) Receiver operating characteristic curve evaluating the global performance of the final model on an independent testing subset. Negative: hypertension absent; positive: hypertension present; AUC: area under the curve.

mixed, inconsistent and less effective contribution of these metrics to the model prediction. On average, the contribution of REMOV to hypertension prediction was approximatively twice that of PSG_ORDI, PSG_AHI or ODI.

The ranking of predictive features was consistent in Ridge logistic regression analysis, which confirmed the important association between increased respiratory effort and the risk of hypertension (supplementary figure S2). Increased respiratory effort for >60% of the night remained an independent predictor of hypertension even in the absence of oxygen desaturation and when sleep fragmentation was limited (supplementary figure S3).

Discussion

The novel finding of this study was that increased respiratory effort detected by MJM analysis was independently and strongly associated with prevalent hypertension in a large clinical cohort of patients with OSA. Respiratory effort burden was a stronger predictor of hypertension than common PSG-derived metrics such as the AHI. While increased respiratory effort was not the only, or the strongest, predictor of hypertension in patients with OSA, the current data provide a more comprehensive picture of the intermediary mechanisms and factors contributing to the development of hypertension in this patient group.

There is a pathophysiological rationale for the observed association between increased respiratory effort during sleep and hypertension. Obstructive events during sleep are the consequence of partial or complete collapse of the upper airway. These alterations in upper airway patency result in repetitive forced inspiration against the obstructed upper airway with substantial negative changes in intrathoracic pressures [20, 23]. These large intrathoracic pressure swings not only generate sympathetic activation but also generate significant shear stress and vessel wall remodelling. The impact of increased respiratory effort has been poorly studied and is probably underestimated as a risk factor for OSA-related hypertension. The current findings showed that respiratory effort load was an independent predictor of prevalent hypertension
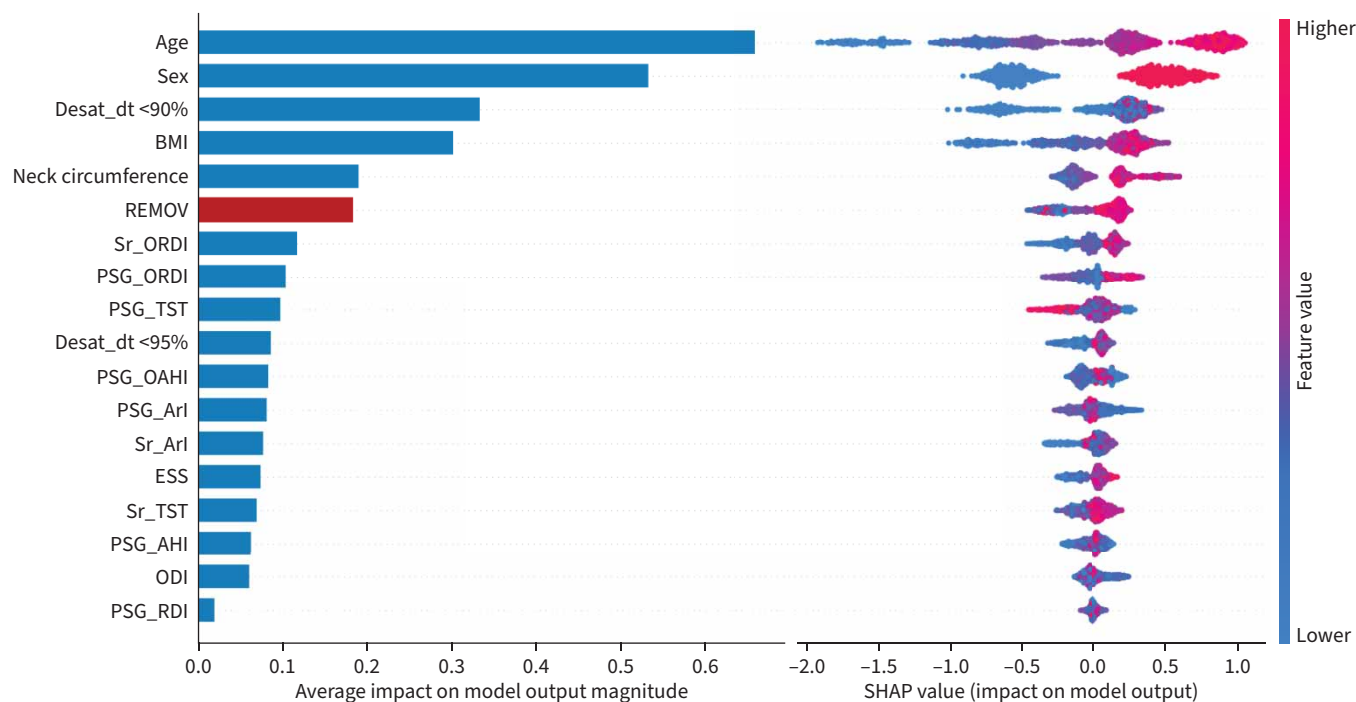
FIGURE 5 Contribution of the 18 input features to the classification output, evaluated by the Shapley additive explanation (SHAP) method. The bar graph on the left compares the average impact of a feature on model output magnitude. Each bar indicates the average of absolute SHAP values for a specific feature in all individual cases. For the graph on the right, the x-axis represents the SHAP value scale, which is proportional to the probability of having hypertension. Each dot indicates the feature attribution value to the extreme gradient boosting model final prediction score for a respective patient. The dots are coloured according to the relative value of a specific feature, in which blue (cooler) or red (warmer) dots represent lower or higher feature values, respectively. AHI: apnoea–hypopnoea index; ArI: arousal index; BMI: body mass index; Desat_dt <90% or <95%: proportion of TST spent with peripheral oxygen saturation <90% or <95%; ESS: Epworth Sleepiness Scale; OAHI: obstructive apnoea–hypopnoea index; ODI: oxygen desaturation index; ORDI: obstructive respiratory disturbance index; PSG_: derived from polysomnography; RDI: respiratory disturbance index; REMOV: proportion of total sleep time with increased respiratory effort during sleep (based on mandibular jaw movements (MJM) measurement); Sr_: derived from automatic analysis of MJM by the Sunrise system; TST: total sleep time.

in OSA beyond intermittent hypoxia. Therefore, we suggest the utility of a pragmatic tool using MJM for objectively measuring sleep time spent with increased respiratory effort. This seems like the most appropriate tool given that increased respiratory effort is poorly documented by respiratory bands, with clear overestimation of central events in obese patients [35]. Snoring is a qualitative and indirect surrogate of increased respiratory effort, and inspiratory flow limitation reflects an increase in upper airway resistance. However, there is not a linear relationship between increase in respiratory effort and flattening of the inspiratory curve [36].

Based on indirect assessment of respiratory effort-related snoring or flow limitation, it has been suggested that increased nocturnal respiratory effort may play a role in the occurrence of hypertension in several different clinical scenarios, including upper airway resistance syndrome (UARS), OSA in children and pre-eclampsia [37–39]. In UARS, measures of nasal flow limitation have been associated with hypertension independently of the AHI [37, 40]. Also, several studies have postulated that snoring and RERAs are associated with significant daytime sleepiness and have repercussions in cardiovascular risk [37, 41, 42]. In these situations, hypoxic burden is limited and treatment indications for continuous positive airway pressure (CPAP) or oral appliances are still the subject of debate. Reliable and convenient assessment of respiratory effort burden throughout the night might allow better risk stratification and personalised treatment solutions in these contexts.

Beyond suppression of intermittent hypoxia and apnoeas/hypopnoeas, the goal of CPAP titration is the full normalisation of respiratory effort, allowing complete restoration of the sleep architecture [37, 43]. This effect contributes to the suppression of persistent sleepiness during CPAP therapy [43] and our study suggests that this might be necessary to improve blood pressure control in patients with OSA. Prospective evaluation of the effects of CPAP therapy on blood pressure in patients with evidence of increased

respiratory effort but without significant oxygen desaturations or sleep fragmentation would also be an interesting area for future research.

Large intrathoracic pressure swings related to increased respiratory effort particularly affect intrathoracic blood vessels, including the aorta. Increased respiratory effort not only favours the development of hypertension, as shown in our study, but might in the long run trigger or exacerbate the progression of aortic dilatation [44]. In addition, a recent meta-analysis suggested an association between OSA and aortic enlargement [45]. Increased respiratory effort is probably a major contributor to this association and the risk is particularly relevant in at-risk populations such as those with previous aortic dissection [46–48]. Better control of diurnal and nocturnal hypertension [49] and the reduction of intrathoracic pressure swings might help to slow the progression of aortic dilation in patients with concomitant OSA.

Our study was conducted in a large consecutive prospective sample covering the broad spectrum of OSA. This suggests that our results have good external validity, but additional validation in other cohorts is desirable. Previous studies in the field have been conducted using less reliable measurement of respiratory effort, *i.e.* snoring and flow limitation. In contrast, our quantitative and direct estimation of respiratory effort level with MJM analytics has been validated against PSG [33] and provides a new metric indicating the total respiratory effort load during sleep. Although an association between increased respiratory effort and hypertension was documented, we do not have 24-h ambulatory blood pressure data and so cannot determine whether increased nocturnal respiratory effort is specifically associated with nocturnal hypertension.

In conclusion, our study highlights the underestimated role of increased respiratory effort as a risk factor for prevalent hypertension in OSA. Respiratory effort load is an independent risk factor for hypertension beyond classical anthropometric cardiovascular risk factors and usual PSG metrics. Risk stratification using new metrics beyond AHI is the new paradigm in OSA [49], and our data suggest that increased respiratory effort based on measurement of MJM, allowing objective measurement of sleep time spent with increased respiratory effort, should be included in the range of new indices for OSA management. This measurement is of particular interest in specific populations such as those with UARS without desaturations or in patients with cardiovascular diseases at high risk for aortic expansion and dissection. A digital medicine solution incorporating MJM and artificial intelligence analysis is ready to operate with home recordings over multiple nights of evaluation, before and after therapeutic interventions.

References

1   Benjafield AV, Ayas NT, Eastwood PR, *et al.* Estimation of the global prevalence and burden of obstructive sleep apnoea: a literature-based analysis. *Lancet Respir Med* 2019; 7: 687–698.

2   Jennum P, Coaquira Castro J, Mettam S, *et al.* Socioeconomic and humanistic burden of illness of excessive daytime sleepiness severity associated with obstructive sleep apnoea in the European Union 5. *Sleep Med* 2021; 84: 46–55.

3   Alomri RM, Kennedy GA, Wali SO, *et al.* Association between nocturnal activity of the sympathetic nervous system and cognitive dysfunction in obstructive sleep apnoea. *Sci Rep* 2021; 11: 11990.

4   Linz D, Woehrle H, Bitter T, *et al.* The importance of sleep-disordered breathing in cardiovascular disease. *Clin Res Cardiol* 2015; 104: 705–718.

5   Lavie P, Herer P, Hoffstein V. Obstructive sleep apnoea syndrome as a risk factor for hypertension: population study. *BMJ* 2000; 320: 479–482.

6   Nieto FJ, Young TB, Lind BK, *et al.* Association of sleep-disordered breathing, sleep apnea, and hypertension in a large community-based study. Sleep Heart Health Study. *JAMA* 2000; 283: 1829–1836.

7   Peppard PE, Young T, Palta M, *et al.* Prospective study of the association between sleep-disordered breathing and hypertension. *N Engl J Med* 2000; 342: 1378–1384.

8   Kohler M, Stradling JR. Mechanisms of vascular damage in obstructive sleep apnea. *Nat Rev Cardiol* 2010; 7: 677–685.

9   Azarbarzin A, Sands SA, Stone KL, *et al.* The hypoxic burden of sleep apnoea predicts cardiovascular disease-related mortality: the Osteoporotic Fractures in Men Study and the Sleep Heart Health Study. *Eur Heart J* 2019; 40: 1149–1157.

10   Butler MP, Emch JT, Rueschman M, *et al.* Apnea–hypopnea event duration predicts mortality in men and women in the sleep heart health study. *Am J Respir Crit Care Med* 2019; 199: 903–912.

11   Lévy P, Tamisier R, Pépin JL. Assessment of sleep-disordered-breathing: quest for a metric or search for meaning? *J Sleep Res* 2020; 29: e13143.

12   Malhotra A, Ayappa I, Ayas N, *et al.* Metrics of sleep apnea severity: beyond the apnea–hypopnea index. *Sleep* 2021; 44: zsab030.

13   Ryan S. Mechanisms of cardiovascular disease in obstructive sleep apnoea. *J Thorac Dis* 2018; 10: S4201–S4211.

14   Weiss JW, Remsburg S, Garpestad E, *et al.* Hemodynamic consequences of obstructive sleep apnea. *Sleep* 1996; 19: 388–397.

15   Ali NJ, Davies RJ, Fleetham JA, *et al.* The acute effects of continuous positive airway pressure and oxygen administration on blood pressure during obstructive sleep apnea. *Chest* 1992; 101: 1526–1532.

16   Berry RB, Asyali MA, McNellis MI, *et al.* Within-night variation in respiratory effort preceding apnea termination and EEG delta power in sleep apnea. *J Appl Physiol* 1998; 85: 1434–1441.

17   Fletcher EC. The relationship between systemic hypertension and obstructive sleep apnea: facts and theory. *Am J Med* 1995; 98: 118–128.

18   Hoffstein V, Chan CK, Slutsky AS. Sleep apnea and systemic hypertension: a causal association review. *Am J Med* 1991; 91: 190–196.

19   Issa FG, Sullivan CE. Upper airway closing pressures in snorers. *J Appl Physiol Respir Environ Exerc Physiol* 1984; 57: 528–535.

20   Magder SA, Lichtenstein S, Adelman AG. Effect of negative pleural pressure on left ventricular hemodynamics. *Am J Cardiol* 1983; 52: 588–593.

21   Peters J, Kindred MK, Robotham JL. Transient analysis of cardiopulmonary interactions. I. Diastolic events. *J Appl Physiol* 1988; 64: 1506–1517.

22   Peters J, Kindred MK, Robotham JL. Transient analysis of cardiopulmonary interactions. II. Systolic events. *J Appl Physiol* 1988; 64: 1518–1526.

23   Sforza E, Krieger J, Petiau C. Nocturnal evolution of respiratory effort in obstructive sleep apnoea syndrome: influence on arousal threshold. *Eur Respir J* 1998; 12: 1257–1263.

24   Stradling JR, Barbour C, Glennon J, *et al.* Which aspects of breathing during sleep influence the overnight fall of blood pressure in a community population? *Thorax* 2000; 55: 393–398.

25   Young T, Finn L, Hla KM, *et al.* Snoring as part of a dose-response relationship between sleep-disordered breathing and blood pressure. *Sleep* 1996; 19: S202–S205.

26   Martinot JB, Le-Dong NN, Cuthbert V, *et al.* Mandibular movements as accurate reporters of respiratory effort during sleep: validation against diaphragmatic electromyography. *Front Neurol* 2017; 8: 353.

27   Pepin JL, Le-Dong NN, Cuthbert V, *et al.* Mandibular movements are a reliable noninvasive alternative to esophageal pressure for measuring respiratory effort in patients with sleep apnea syndrome. *Nat Sci Sleep* 2022; 14: 635–644.

28   Berry RB, Brooks R, Gamaldo C, *et al.* AASM Scoring Manual updates for 2017 (Version 2.4). *J Clin Sleep Med* 2017; 13: 665–666.

29   Berry RB, Budhiraja R, Gottlieb DJ, *et al.* Rules for scoring respiratory events in sleep: update of the 2007 AASM manual for the scoring of sleep and associated events. Deliberations of the Sleep Apnea Definitions Task Force of the American Academy of Sleep Medicine. *J Clin Sleep Med* 2012; 8: 597–619.

30   American Academy of Sleep Medicine. International Classification of Sleep Disorders. 3rd Edn. Darien, AASM, 2014.

31   Martinot JB, Borel JC, Cuthbert V, *et al.* Mandibular position and movements: suitability for diagnosis of sleep apnoea. *Respirology* 2017; 22: 567–574.

32   Le-Dong NN, Martinot JB, Coumans N, *et al.* Machine learning-based sleep staging in patients with sleep apnea using a single mandibular movement signal. *Am J Respir Crit Care Med* 2021; 204: 1227–1231.

33   Pépin JL, Letesson C, Le-Dong NN, *et al.* Assessment of mandibular movement monitoring with machine learning analysis for the diagnosis of obstructive sleep apnea. *JAMA Netw Open* 2020; 3: e1919657.

34   Lundberg SM, Erion G, Chen H, *et al.* From local explanations to global understanding with explainable AI for trees. *Nat Mach Intell* 2020; 2: 56–67.

35   Boudewyns A, Willemen M, Wagemans M, *et al.* Assessment of respiratory effort by means of strain gauges and esophageal pressure swings: a comparative study. *Sleep* 1997; 20: 168–170.

36   Pamidi S, Redline S, Rapoport D, *et al.* An official American Thoracic Society workshop report: noninvasive identification of inspiratory flow limitation in sleep studies. *Ann Am Thorac Soc* 2017; 14: 1076–1085.

37   Pépin JL, Guillot M, Tamisier R, *et al.* The upper airway resistance syndrome. *Respiration* 2012; 83: 559–566.

38   Guilleminault C, Winkle R, Korobkin R, *et al.* Children and nocturnal snoring: evaluation of the effects of sleep related respiratory resistive load and daytime functioning. *Eur J Pediatr* 1982; 139: 165–171.

39   Edwards N, Blyton DM, Kirjavainen T, *et al.* Nasal continuous positive airway pressure reduces sleep-induced blood pressure increments in preeclampsia. *Am J Respir Crit Care Med* 2000; 162: 252–257.

40   Guilleminault C, Stoohs R, Shiomi T, *et al.* Upper airway resistance syndrome, nocturnal blood pressure monitoring, and borderline hypertension. *Chest* 1996; 109: 901–908.

41   Asker M, Asker S, Kucuk U, *et al.* An overlooked cause of resistant hypertension: upper airway resistance syndrome – preliminary results. *Clinics* 2014; 69: 731–734.

42   Guilleminault C, Kirisoglu C, Poyares D, *et al.* Upper airway resistance syndrome: a long-term outcome study. *J Psychiatr Res* 2006; 40: 273–279.

43   Meurice JC, Paquereau J, Denjean A, *et al.* Influence of correction of flow limitation on continuous positive airway pressure efficiency in sleep apnoea/hypopnoea syndrome. *Eur Respir J* 1998; 11: 1121–1127.

44   Gaisl T, Bratton DJ, Kohler M. The impact of obstructive sleep apnoea on the aorta. *Eur Respir J* 2015; 46: 532–544.

45   Gherbesi E, Tadic M, Faggiano A, *et al.* Sleep apnea syndrome and large artery subclinical damage: targeting thoracic aortic dilatation. *Am J Hypertens* 2022; 35: 543–550.

46   Barone-Rochette G, Thony F, Boggetto-Graham L, *et al.* Aortic expansion assessed by imaging follow-up after acute aortic syndrome: effect of sleep apnea. *Am J Respir Crit Care Med* 2015; 192: 111–114.

47   Delsart P, Soquet J, Pierache A, *et al.* Influence of nocturnal hypoxemia on follow-up course after type B acute aortic syndrome. *BMC Pulm Med* 2021; 21: 401.

48   Delsart P, Soquet J, Drumez E, *et al.* Aortic root size is associated with nocturnal blood pressure in a population of hypertensive patients under treatment for obstructive sleep apnea. *Sleep Breath* 2019; 23: 439–446.

49   Pépin J-L, Eastwood P, Eckert DJ. Novel avenues to approach non-CPAP therapy and implement comprehensive obstructive sleep apnoea care. *Eur Respir J* 2022; 59: 2101788.